Bioactive Stratified Polymer Ceramic-Hydrogel Scaffold for Integrative Osteochondral Repair

JIE JIANG,[1] AMY TANG,[1] GERARD A. ATESHIAN,[2] X. EDWARD GUO,[3] CLARK T. HUNG,[4] and HELEN H. LU[1,5]

[1]Biomaterials and Interface Tissue Engineering Laboratory, Department of Biomedical Engineering, Columbia University, 351 Engineering Terrace Building, MC 8904, 1210 Amsterdam Avenue, New York, NY 10027, USA; [2]Musculoskeletal Biomechanics Laboratory, Departments of Biomedical and Mechanical Engineering, Columbia University, New York, NY 10027, USA; [3]Bone Bioengineering Laboratory, Department of Biomedical Engineering, Columbia University, New York, NY 10027, USA; [4]Cellular Engineering Laboratory, Department of Biomedical Engineering, Columbia University, New York, NY 10027, USA; and [5]College of Dental Medicine, Columbia University, New York, NY 10032, USA

Associate Editor Michael S. Detamore oversaw the review of this article.

Abstract—Due to the intrinsically poor repair potential of articular cartilage, injuries to this soft tissue do not heal and require clinical intervention. Tissue engineered osteochondral grafts offer a promising alternative for cartilage repair. The functionality and integration potential of these grafts can be further improved by the regeneration of a stable calcified cartilage interface. This study focuses on the design and optimization of a stratified osteochondral graft with biomimetic multi-tissue regions, including a pre-designed and pre-integrated interface region. Specifically, the scaffold based on agarose hydrogel and composite microspheres of polylactide-*co*-glycolide (PLGA) and 45S5 bioactive glass (BG) was fabricated and optimized for chondrocyte density and microsphere composition. It was observed that the stratified scaffold supported the region-specific co-culture of chondrocytes and osteoblasts which can lead to the production of three distinct yet continuous regions of cartilage, calcified cartilage and bone-like matrices. Moreover, higher cell density enhanced chondrogenesis and improved graft mechanical property over time. The PLGA-BG phase promoted chondrocyte mineralization potential and is required for the formation of a calcified interface and bone regions on the osteochondral graft. These results demonstrate the potential of the stratified scaffold for integrative cartilage repair and future studies will focus on scaffold optimization and *in vivo* evaluations.

Keywords—Osteochondral, Tissue engineering, Bioactive glass, Interface, Hydrogel, Microsphere.

Address correspondence to Helen H. Lu, Biomaterials and Interface Tissue Engineering Laboratory, Department of Biomedical Engineering, Columbia University, 351 Engineering Terrace Building, MC 8904, 1210 Amsterdam Avenue, New York, NY 10027, USA. Electronic mail: hl2052@columbia.edu

INTRODUCTION

Arthritis is the leading cause of disability among Americans,[44] and the most common form of arthritis is osteoarthritis, with 21 million Americans suffering from this degenerative condition.[44] Injury to articular cartilage is a major contributor to the onset of osteoarthritis.[20,82] Due to the limited regenerative capacity of adult articular cartilage, surgical intervention is often required. Existing treatment options have achieved variable degrees of success for the repair of focal lesions and damage to the articular surface.[37,68] These methods include abrasion arthroplasty,[2,76] Pridie drilling,[8] microfracture,[77] autogenous or allogeneic cell/tissue transfer via periosteal grafts,[58] tissue adhesives,[1,28] and autologous osteochondral grafts.[26,50] For the treatment of large osteochondral defects, one of the options is autologous osteochondral grafts such as those used in mosaicplasty.[26,37,68] These autografts show good initial results, but are limited by donor site morbidity and functional incompatibility between the host and donor tissue, which can compromise long term graft outcome.

Tissue engineered cartilage has emerged as an alternative treatment option for cartilage lesions. Several groups have reported on the development of tissue engineered osteochondral grafts[3–6,17,21,23–25,27,33,34,39,57,59,70–75,78,79,83] that have demonstrated significant potential. Most of these osteochondral grafts use a stratified scaffold design that facilitates the development of both cartilaginous and bony regions. The first generation of stratified scaffolds consisted of two different scaffold phases each representing the cartilage or bone regions, joined together with either sutures or sealants.[24,71]

Schaefer et al.[71] seeded bovine articular chondrocytes on polyglycolic acid (PGA) meshes and periosteal cells on poly(lactic-co-glycolic acid) (PLGA)/polyethylene glycol foams, and subsequently sutured the separate constructs together at one or four weeks after seeding. Shortly after, Sherwood et al.[75] developed a continuous stratified scaffold using the TheriForm™ three-dimensional printing process. An osteochondral graft with a transition region of varied porosity and composition between a cartilage region and a bone region was formed. These pioneering studies of stratified osteochondral grafts demonstrate the feasibility of engineering multi-tissue formation on a multi-phased scaffold. Potential challenges that these grafts face include maintaining the stability of the cartilage and bone regions, as well as the integration of the graft with the host tissue. One area of special importance in osteochondral graft design that has often been understudied is the regeneration of the osteochondral interface, which will be critical for graft integration and for establishing long-term functionality.

The native osteochondral interface is comprised of a thin layer of mineralized cartilage that bridges bone and cartilage, with the tidemark demarcating the hyaline articular cartilage from the calcified cartilage region.[13,22,29,49,62,64] The tidemark and the calcified cartilage layer collectively constitute the osteochondral interface, which facilitates the pressurization and physiological loading of articular cartilage while functioning as a physical barrier for vascular invasion from subchondral bone.[19,54,67] Advancement of the calcified region towards the articular surface is observed with age,[30,42,43,60,62] and has been associated with osteoarthritis.[11,12,14,61,63,65] According to Collins, the absence of a stable calcified cartilage interface between the cartilage proper and vascular bone, whether in a joint, an intervertebral disc or a rib, indicates that the interface is temporary, unstable and often pathological.[19] Hunziker et al.[35,36] elegantly demonstrated that a physical barrier is essential for maintaining the stability of the neo-cartilage formed post repair and would prevent unwanted bony ingrowth. Therefore, the next stage in osteochondral graft design must take into consideration the regeneration of the osteochondral interface or a calcified cartilage layer between the cartilage and bone regions.

The ideal osteochondral graft for the treatment of articular cartilage defects needs to match the mechanical and functional properties of the native tissue as well as accommodate structural requirements such as size and surface contour under various load-bearing conditions. In addition to supporting chondrogenesis, it needs to functionally integrate with the host tissue including both surrounding cartilage and subchondral bone. Our approach is to engineer a multi-phased osteochondral graft by combining existing cartilage and bone grafts that have the ability to meet all the mechanical and functional properties of the native tissue while focusing on the formation of a functional interface between the cartilage and bone regions in vitro. The design of this graft encompasses a stratified scaffold system comprised of three sections intended for the formation of three distinct yet continuous tissue regions: cartilage, interface, and bone.

Specifically in this study, a multi-phased scaffold of hydrogel and sintered microspheres of polymer–ceramic composite has been formed (Fig. 1). The cartilage phase of the osteochondral graft is based on the thermal setting agarose hydrogel (G) that has been shown to exhibit physiologically relevant mechanical properties,[45] supporting the formation of functional cartilage-like matrix in vitro[15,16,51] and in vivo.[56] Moreover, agarose hydrogel have been used extensively in chondrocyte biology.[18,69] The bone region of the scaffold consists of polylactide-co-glycolide (PLGA) and 45S5 bioactive glass (BG) composite microspheres (PLGA-BG) sintered together to form a 3-D
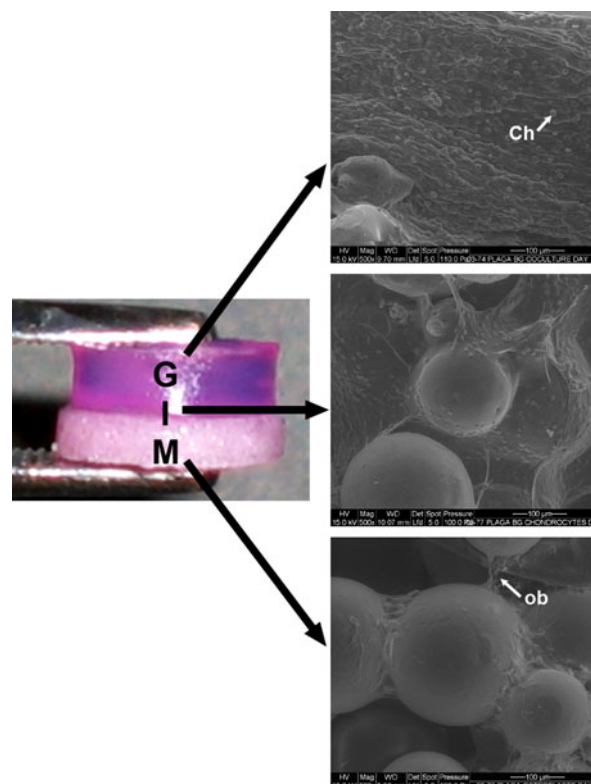

FIGURE 1. Multi-phased osteochondral scaffold. The stratified scaffold consisted of pre-integrated hydrogel (G), hydrogel + microsphere interface (I) and microsphere (M) bone regions (ESEM, day 10, 500×). Note the spherical chondrocytes (C) within the hydrogel, and agarose can be seen to penetrate into the pores of the microsphere phase at the interface region (I). Elongated osteoblasts are observed in the microspheres-only region (M).

interconnected microsphere phase (M). This PLGA-BG composite has been shown to be biodegradable and osteointegrative, as it forms surface calcium phosphate deposits in a simulated body fluid, and in the presence of cells and serum proteins *in vitro*.[10,46,48] In addition, the PLGA-BG composite exhibits improved mechanical properties and osteointegrative potential compared to microsphere scaffolds of PLGA alone.[46] The interface region (I) of the stratified scaffold consists of a hybrid phase of the agarose hydrogel and the sintered PLGA-BG microspheres, designed to promote the formation of a calcified cartilage region that is pre-integrated with the aforementioned agarose-based cartilage and PLGA-BG-based bone regions.

The objective of this study is to optimize the design of this multi-phased osteochondral graft, focusing on (1) the effects of chondrocyte density on matrix production and on mechanical properties of the cartilage region as well as (2) the effects of the BG phase of the PLGA-BG composite on chondrocyte mineralization potential and the formation of a calcified cartilage region. Published reports have shown that higher chondrocyte density in tissue engineered agarose constructs results in enhanced graft mechanical properties.[51,52] Moreover, the effects of bioactive and osteointegrative ceramics such as BG on chondrocyte response are not well understood, and it is hypothesized that PLGA-BG will promote chondrocyte mineralization and thus facilitate the formation of a calcified cartilage matrix on the interface region of the stratified scaffold.

Another important consideration in designing a tissue engineered osteochondral graft is the interaction between the different cell types, such as chondrocytes and osteoblasts.[38] This is particularly relevant as multiple tissue types and hence multiple cell types are inherent in the osteochondral graft and their contribution to osteochondral tissue formation and the stability of each tissue region have been mostly understudied. These heterotypic cellular interactions may play an important role in the formation of distinct yet continuous tissue regions, initiating the events that lead to regeneration of the osteochondral interface. Therefore, the third objective of this study is to establish co-culture of chondrocytes and osteoblasts on the multi-phased osteochondral graft, with chondrocytes-only in the agarose layer, chondrocytes-only in the agarose-PLGA-BG hybrid layer and osteoblasts-only in the PLGA-BG layer. It is hypothesized that the region-specific distribution of chondrocytes and osteoblasts on the stratified scaffold would lead to the formation of three distinct yet continuous regions of cartilage (G), calcified cartilage (I) and bone-like matrix (M) *in vitro*. It is anticipated that successful regeneration of an osteochondral graft with a calcified cartilage interface will extend graft functionality and

ensure long-term clinical success. Moreover, the multi-phasic scaffold design principles and co-culturing methodologies tested in this study would lead to the development of a new generation of integrative osteochondral graft for the treatment of osteoarthritis.

MATERIAL AND METHODS

Cells and Cell Culture

Primary articular chondrocytes and osteoblasts were used in this study. Specifically, articular chondrocytes were isolated aseptically from the carpometacarpal joints of 1–4 weeks old calves through enzymatic digestion following published methods.[38] Briefly, hyaline cartilage was excised from the exposed articular joint surface and minced into small pieces. Articular chondrocytes were subsequently obtained following serial enzymatic digestions of the isolated cartilage, first with 0.25% w/v protease (Calbiochem, San Diego, CA) in serum-free Dulbecco's Modified Eagles Medium (DMEM, Cellgro-Mediatech, Herndon, VA) for one hour, followed by a 4-h digestion with 0.05% w/v collagenase (Sigma-Aldrich, St. Louis, MO) in DMEM. After digestion, the cell suspension was filtered with a 30 μm mesh (Spectrum, Rancho Dominguez, CA). The isolated chondrocytes were then resuspended and maintained in fully supplemented DMEM with 10% fetal bovine serum (Atlanta Biologic, Atlanta, GA), 1% P/S (10,000 I.U. penicillin, 10,000 μg/mL streptomycin) and 1% non-essential amino acid (all purchased from Cellgro-Mediatech).

Primary cultures of bovine osteoblast-like cells were derived from explants of bone fragments taken from the same joints as the cartilage, following published protocols.[80] Briefly, bone fragments were excised from the tibia using a bone cutter. The fragments were then washed twice with phosphate buffer saline (PBS, Sigma-Aldrich) and placed in a 150 mm^2 flask (BD, Franklin Lakes, NJ) and cultured in fully supplemented DMEM. After 1 week of culture, the bone fragments were transferred to a new plate to obtain the second migration osteoblast-like cells that were used for this study. All cells were maintained in fully supplemented DMEM under humidified conditions at 37 °C and 5% CO_2.

Multi-Phased Osteochondral Scaffold Design

A multi-phased, osteochondral scaffold (Fig. 1) consists of three distinct yet continuous regions mimicking the organization in the native osteochondral interface: a chondrocyte-containing hydrogel phase (G) for cartilage, an interface region (I) consisting of chondrocytes embedded within a hybrid phase of gel

and microspheres, and an osteoblast-only bone region consisting of polymer–ceramic microspheres (M).

The gel-only region representing articular cartilage was formed by encapsulating chondrocytes in sterile 2% agarose (Type VII, low gelling temperature, Sigma-Aldrich) following previously published method.[51] The chondrocyte density in the hydrogel was determined based on the results of the optimization study described below. The microsphere-only bone region was based on a 3-D scaffold of biodegradable polymer or polymer–ceramic composite microspheres formed by a water/oil/water emulsion method.[46] Briefly, poly(DL-lactide-co-glycolide) 85:15 copolymer (PLGA, $M_w \approx 123.6$ kDa, Alkermes, Cambridge, MA) was dissolved in dichloromethane (10% w/v, EM Science, Gibbstown, NJ), then poured into a 1% polyvinyl alcohol (Sigma-Aldrich) solution. To form the polymer–ceramic composite (PLGA-BG) microspheres, a 4:1 mixture of PLGA and 45S5 bioactive glass particles (BG, 20 μm, MO-SCI Corporation Rolla, MD) was used.[46] Both PLGA and PLGA-BG microspheres were subsequently sintered above the polymer glass transition temperature at 55 °C for 20 h in a custom mold to form 3-D interconnected scaffolds (Ø7.5 × 18.5 mm).

The multi-phased scaffold with pre-integrated cartilage, interface and bone regions was fabricated using a custom mold. The chondrocyte-agarose suspension was first cast into the mold, and the microsphere scaffold was then added to the chondrocyte-agarose suspension prior to setting. After the agarose has set, the cartilage and bone regions were connected by the chondrocyte-laden interface region that consisted of hydrogel within the interconnected pores of microsphere scaffold. The multi-phased constructs were then removed from the mold. Osteoblasts were subsequently seeded onto the microsphere-only region of the construct at 200,000 cells/graft following previously published methods[47] and allowed to attach for 15 min before media was added. Total scaffold diameter and thickness were measured following fabrication. Individual phase thickness ($n = 15$) was determined by image analysis (ImageJ, version 1.34s, NIH), while phase diameter ($n = 5$) was measured using a digital caliper. All constructs were maintained in fully supplemented DMEM with 50 μg/mL of ascorbic acid (Sigma-Aldrich) at 5% CO_2 and 37 °C for the duration of the experiment.

Optimizing Chondrocyte Seeding Density in the Cartilage Region

Chondrocyte density in the cartilage region of the osteochondral scaffold was first optimized by evaluating the effect of cell seeding density on matrix deposition and mechanical properties of the hydrogel phase. Briefly, agarose hydrogel containing 10, 20 or 60 million chondrocytes/mL were formed as described above and cultured in fully supplemented DMEM over time. Glycosaminoglycan (GAG), collagen deposition and mechanical properties of the hydrogel region were determined at 10, 20 and 30 days.

Chondrocyte Response to PLGA-BG in the Interface Region

As the chondrocytes at the interface regions will be exposed to PLGA-BG composite, an experiment was first performed to compare the response of chondrocytes on PLGA and PLGA-BG microspheres. Briefly, PLGA or PLGA-BG microspheres were weighed into 48-well plates and sintered at 55 °C for 20 h. After ethanol and UV sterilization, chondrocytes (2.0×10^5 cells/sample) were seeded on the microspheres, and cell proliferation, alkaline phosphatase activity (ALP) and GAG deposition on the microsphere substrates were examined at 1, 7, 14 and 21 days.

Effects of Co-Culture and Microsphere Composition on the Interface and Bone Regions

The effects of co-culturing chondrocytes and osteoblasts on the multi-phased scaffold on the formation of distinct yet continuous cartilage, interface and bone regions were examined over time. Specifically, at days 1, 10 and 20, the constructs were collected and in addition to cell viability and distribution, quantitative and qualitative analysis of both collagen and GAG production were performed to determine matrix deposition in each region (cartilage, interface and bone) of the osteochondral scaffold. Additionally, compressive mechanical properties of the scaffolds under unconfined compression were also measured at 1, 10 and 20 days.

The effects of microsphere composition on the interface and bone regions on matrix deposition in these two regions were examined over time. Osteochondral scaffolds with bony regions containing either PLGA or PLGA-BG microsphere scaffolds were formed. Matrix (collagen, GAG) synthesis and distribution were determined over time via qualitative and quantitative assays, while mineral deposition in the three scaffold regions was evaluated by histology, micro-CT and Energy Dispersive X-ray Analysis (EDAX). Sample ALP activity was also measured over time. Mechanical properties of the constructs under unconfined compression were also examined at 1, 10 and 20 days.

Cell Morphology, Viability and Tracking on the Multi-phased Osteochondral Scaffold

Cell morphology in each region of the multi-phased osteochondral scaffold was examined using environmental scanning electron microscopy (ESEM, 15 kV, FEI, OR). Briefly, at specific time points, the samples were first washed with PBS, then fixed in Karnovsky's fixative and washed again with PBS prior to imaging. In addition, as chondrocytes and osteoblasts were co-cultured on the osteochondral scaffold, in order to visualize the respective localization and migration of each cell type, osteoblasts were pre-labeled with the CM-DiI cell membrane tracking dye (Invitrogen) following the manufacturer's suggested protocol. At designated time points, cell viability was determined with Calcein AM (Invitrogen) using the manufacturer's recommended protocol. The scaffold was then halved and cross sections were visualized under a confocal microscope (Olympus, Melville, NY) at excitation wavelengths of 568 and 488 nm for CM-DiI dye and Calcein AM, respectively.

Cell Proliferation

Total DNA content ($n = 6$) was quantified using the PicoGreen® dsDNA (Invitrogen) assay following the manufacturer's suggested protocol. Briefly, at the designated time points, the samples were collected, washed with PBS, then homogenized and digested overnight at 60 °C in 2% Papain (Sigma-Aldrich) solution. After digestion, 25 μL of the digest was added to 175 μL of PicoGreen® reagent working solution in a 96-well plate. Fluorescence of the samples was measured with a microplate reader (Tecan, Research Triangle Park, NC) with excitation and emission wavelengths of 485 and 535 nm, respectively. The total number of cells in the sample was determined by converting the total DNA to cell number using the conversion of factor of 7.7 pg DNA/cell.[41]

Glycosaminoglycan (GAG) and Collagen Deposition

Glycosaminoglycan content ($n = 6$) was quantified with Blyscan 1,9-dimethylmethylene blue (DMMB) assay kit (Biocolor, UK) using the manufacturer's suggested protocol. Briefly, samples were homogenized and digested in 2% Papain as described above. The digest (100 μL) was then added to 1 mL of the Blyscan assay dye agent and mixed for 1 h. The mixture was then centrifuged for 20 min at 10,000g to isolate the precipitated GAG-dye complex. After removing the supernatant, the precipitate was re-suspended in 1 mL of Blyscan dissociation solution and sample absorbance was measured at 620 nm using a microplate reader (Tecan).

Total collagen content ($n = 6$) was determined by colorimetric hydroxyproline quantification after modifying the method of Reddy et al.[66] Briefly, samples were homogenized and digested in 2% Papain and 10 μL of the sample was mixed with 90 μL of 10 N NaOH, and subsequently hydrolyzed for 30 min at 120 °C. The hydrolyzed solution (50 μL) was then added to 450 μL of 56 mM of chloramines T (Sigma-Aldrich) solution. The oxidation reaction was allowed to proceed for 25 min at room temperature and 500 μL of Ehrlich's reagent was then added to the samples and allowed to incubate for 20 min at 65 °C. Absorbance was read at 550 nm with a microplate reader (Tecan).

Collagen and GAG distribution within each region of the osteochondral scaffold were visualized via histology ($n = 2$). Briefly, the samples were first washed with PBS and fixed in neutral formalin for 30 min, and then embedded in PMMA. Sample sections (10 μM) were used for standard histological analysis. Hematoxylin and eosin was used to visualized cell distribution and morphology, collagen and GAG deposition was visualized using Picrosirius Red and Alcian Blue stain respectively.[38]

Alkaline Phosphatase (ALP) Activity and Mineral Distribution

Cell ALP activity ($n = 6$) was quantified using an enzymatic assay based on the hydrolysis of p-nitrophenyl phosphate (pNP-PO$_4$) to p-nitrophenol (pNP).[81] Briefly, the samples were lysed in 0.1% Triton X solution, then added to pNP-PO$_4$ solution (Sigma-Aldrich) and allowed to react for 30 min at 37 °C. The reaction was terminated with 0.1 N NaOH (Sigma-Aldrich). To examine mineral distribution within each region of the osteochondral scaffold, the samples were first washed with PBS and then fixed in neutral formalin. The specimens were then imaged using a micro-CT (μCT) scanning system (vivaCT 40, SCANCO Medical AG, Switzerland), with the central gage length of 15 mm using an isotropic, nominal resolution of 21 μm. The samples were also stained with Alizarin Red S in order to evaluate mineral deposition within each scaffold region.

Mechanical Property

Equilibrium Young's modulus ($n = 6$) of the tissue engineered osteochondral graft was determined following the methods of Mauck et al.[51] Briefly, samples were subjected to unconfined compression between impermeable platens in a custom mechanical testing device. Constructs were first equilibrated in creep under a tare load of 0.02 N, followed by stress relaxation tests with a ramp displacement of 1 μm/s to 10% strain (based on the post creep thickness of the gel-only

region). The equilibrium Young's modulus was determined from the equilibrium response (2000 s) of the stress-relaxation test.

Statistical Analysis

Results are presented in the form of mean ± standard deviation, with *n* equal to the number of samples analyzed. A two-way analysis of variance (ANOVA) was performed to determine the effects of time, cell seeding density and microsphere composition on total cell number, matrix deposition, ALP activity and mechanical properties. The Tukey–Kramer post-hoc test was used for all pair-wise comparisons, and significance was attained at $p < 0.05$. All statistical analyses were performed using the JMP software (SAS, Cary, NC).

RESULTS

Chondrocyte-Osteoblast Co-Culture on the Multi-phased Osteochondral Graft

As shown in Fig. 1, a multi-phased osteochondral graft with a hydrogel region (G) for cartilage formation, a hydrogel + microsphere interface region (I) for osteochondral interface formation, and a microsphere region (M) for bone formation has been formed. Both gross examination and ESEM imaging revealed that the construct regions were continuous and well integrated with each other. The agarose gel layer penetrated well into the pores of the microsphere scaffolds to form the interface region and construct integrity was maintained over time (Fig. 1). The scaffold phases including the pre-designed interface region remained stable and unchanged in dimension throughout the study.

In terms of cell morphology, it was observed that within the hydrogel layer, the chondrocytes assumed a characteristic spherical morphology, while both spherical and elongated chondrocytes were seen in the interface region, and finally, well spread and elongated osteoblast-like cells were observed in the bone region. These observations were confirmed by cell viability analysis (Fig. 2i). Both chondrocytes and osteoblasts remained viable in the construct for the duration of the culturing period.

Moreover, cell tracking results (Fig. 2ii) revealed that only chondrocytes were found in the hydrogel-based cartilage layer and osteoblasts were only observed in the microsphere-based bone region. Interestingly, while the hybrid hydrogel + microsphere interface region was dominated by chondrocytes (Fig. 2ii), chondrocytes at or near the surface of the hydrogel did attach onto the microspheres in the interface region. These observations were confirmed as the elongated cells observed at the interface region, unlike osteoblasts, did not stain positively for the CM-DiI cell tracking dye (Fig. 2ii).

Optimizing Chondrocyte Seeding Density in the Cartilage Region

Total DNA was determined in this study, with the highest DNA content consistently found in the 60 million/mL group at all time points examined (Fig. 3i). Over time, a moderate decrease in DNA content was evident in all hydrogel groups. As shown in Fig. 3, by increasing chondrocyte density in the hydrogel, a significant increase in total collagen content was
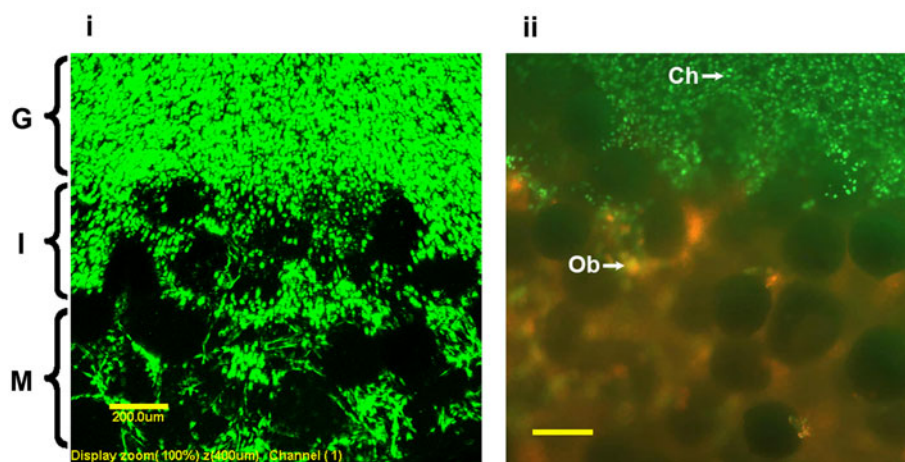

FIGURE 2. Cell viability and chondrocyte-osteoblast co-culture: (i) viability stain of the osteochondral graft confirms cell viability and reveals region-specific cell morphology (10×, day 10); (ii) chondrocytes (*green*) and osteoblasts (*green*) at the interface region (Calcein stain overlay CM-DiI dye, 5×, day 10).
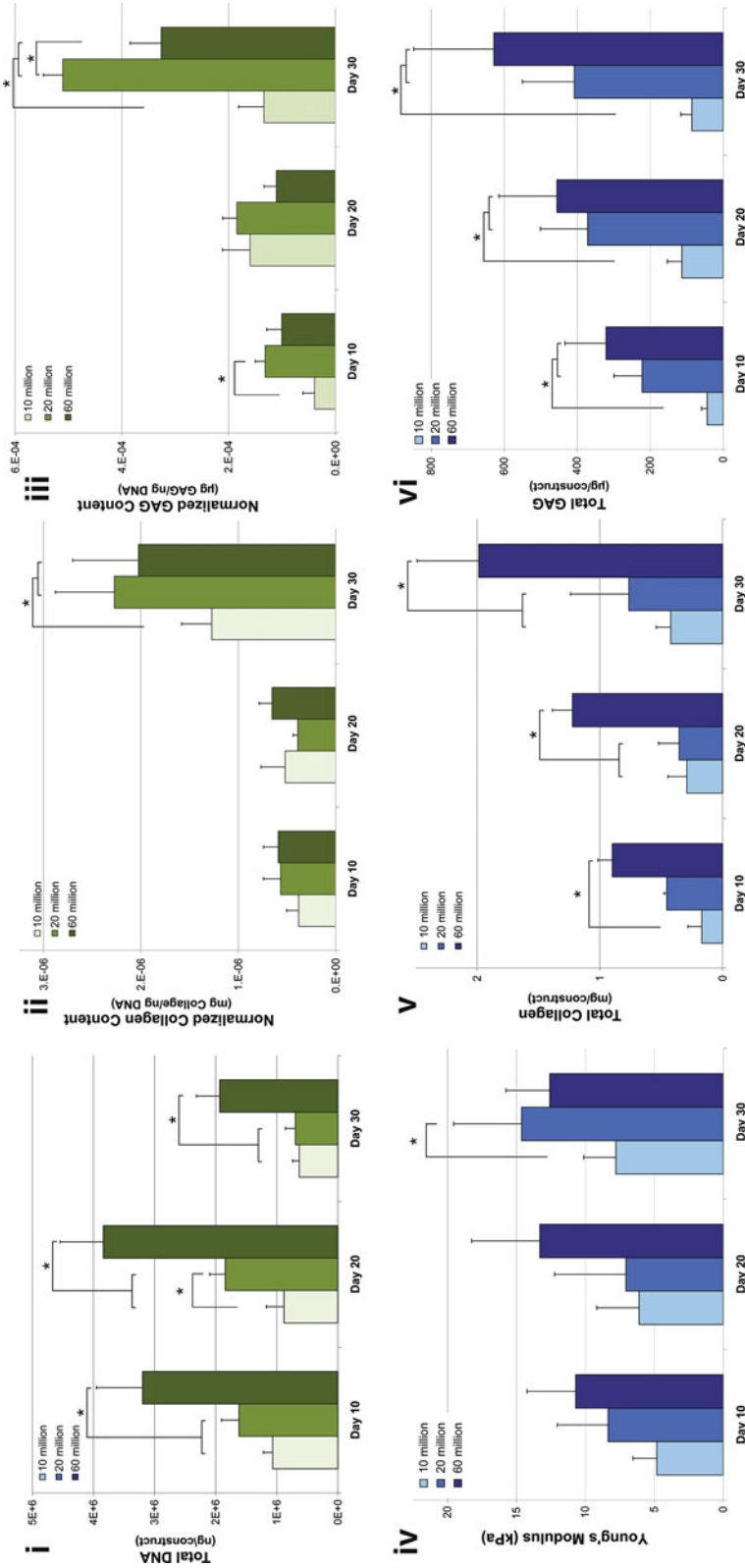
FIGURE 3. Effects of chondrocyte density on biosynthesis and mechanical property. Total DNA content (i) decreased moderately over time in all hydrogel groups, with the highest level found in the 60 million/mL group. Both Collagen (ii, v) and GAG (iii, vi) deposition increased in all groups over time. Collagen content increased with higher chondrocyte density. Similarly, total GAG increased with cell density, with comparable GAG levels found for the 20 million/mL and 60 million/mL groups. Mechanical properties (iv) also increased with higher chondrocyte density (* $p < 0.05$).

observed over 30 days of culture (Figs. 3ii and 3v). When collagen deposition was normalized with total DNA, the 20 million/mL and 60 million/mL groups measured a comparable level of collagen content at all time points examined (Fig. 3ii). The highest total collagen deposition was found in the 60 million/mL group at day 30, with significant differences detected between the 60 million/mL and the 10 or 20 million/mL groups at all time points tested ($p < 0.05$, Fig. 3v).

Similarly, total GAG content was the highest in the 60 million/mL group, with significant differences detected between the 60 and 10 million/mL groups at all three time points tested ($p < 0.05$, Fig. 3vi). When GAG content was normalized with DNA content, the 20 million/mL group showed the highest GAG deposition/cell by day 30 (Fig. 3iii). In terms of mechanical properties, while no difference in Young's modulus was found between the three seeding densities at 10 or 20 days, a significantly higher modulus was detected in the 20 million/mL group compared to 10 million/mL group at day 30 ($p < 0.05$, Fig. 3iv), with no significant difference seen between the 20 and 60 million/mL groups at the same time point. Due to the significant increase in total matrix deposition, all subsequent studies were performed using the 60 million/mL seeding density in the cartilage region.

Chondrocyte Response to PLGA-BG in the Interface Region

The response of chondrocytes on PLGA-BG microspheres was compared to those of PLGA. It was observed that the ALP activity of chondrocytes peaked at day 7, and increased significantly when cultured on PLGA-BG scaffolds ($p < 0.05$, Fig. 4i), while only a basal level of enzyme activity was observed on PLGA scaffolds without BG. Moreover, chondrocyte GAG production was also significantly higher on PLGA-BG when compared to PLGA microspheres, with significant differences detected at day 14, 21 and 28 ($p < 0.05$, Fig. 4ii).

Characterization of Matrix Deposition and Mechanical Properties

Matrix synthesis and distribution on the multiphased osteochondral graft co-culture model was determined over time. Total collagen content increased over time on the osteochondral scaffold ($p < 0.05$, Fig. 5i), and based on histological assessment, collagen distribution was relatively uniform on all three regions (G, I, M) of the scaffold (Fig. 5ii). Similarly, GAG content also increased significantly over time on the osteochondral graft ($p < 0.05$, Fig. 6i), however, histological staining revealed that GAG deposition was
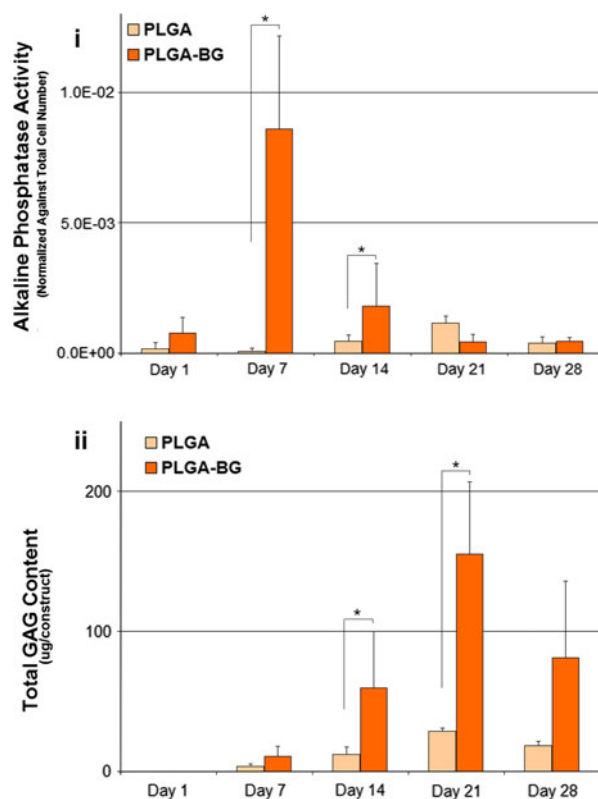

FIGURE 4. Effects of microsphere composition on chondrocyte response. (i) ALP activity of chondrocytes peaked at day 7 and increased on PLGA-BG over PLGA control (* $p < 0.05$). (ii) Glycosaminoglycan (GAG) production also increased significantly on PLGA-BG over PLGA control (* $p < 0.05$).

limited to the cartilage (G) and interface (I) layers, with no positive staining observed in the bone (M) region (Fig. 6ii).

Equilibrium modulus of the construct increased significantly with culturing time ($p < 0.05$, Fig. 7i). Specifically, the scaffold Young's modulus averaged 20 kPa at day 20, and due to the testing configuration (10% strain) utilized, it represents largely the modulus of only the hydrogel region. This observation was confirmed with the modulus of the gel-only region after the three scaffold regions were separated.

Effects of Composition on the Interface and Bone Regions (PLGA vs. PLGA-BG)

The effects of microsphere composition on the multiphased osteochondral graft were determined. There were no significant differences in either collagen (Fig. 5) or GAG (Fig. 6) deposition or distribution between the osteochondral grafts made with PLGA or PLGA-BG microspheres. The equilibrium moduli of the two scaffolds were also comparable (Fig. 7), with no significant difference found at all culturing times examined.
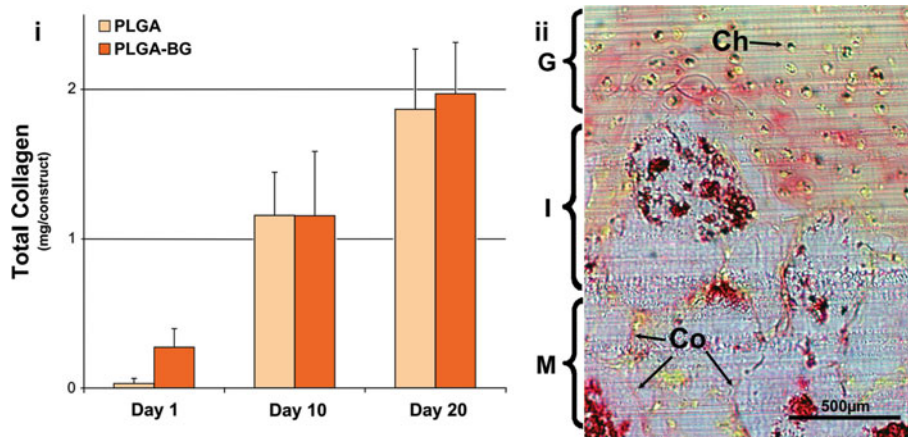
FIGURE 5. Collagen deposition in stratified osteochondral scaffold. (i) Total collagen deposition increased with time with no significant difference found between PLGA and PLGA-BG groups. (ii) Collagen (Co) deposition was evident throughout the scaffold phases (Picrosirius Red, Day 10; 20×).
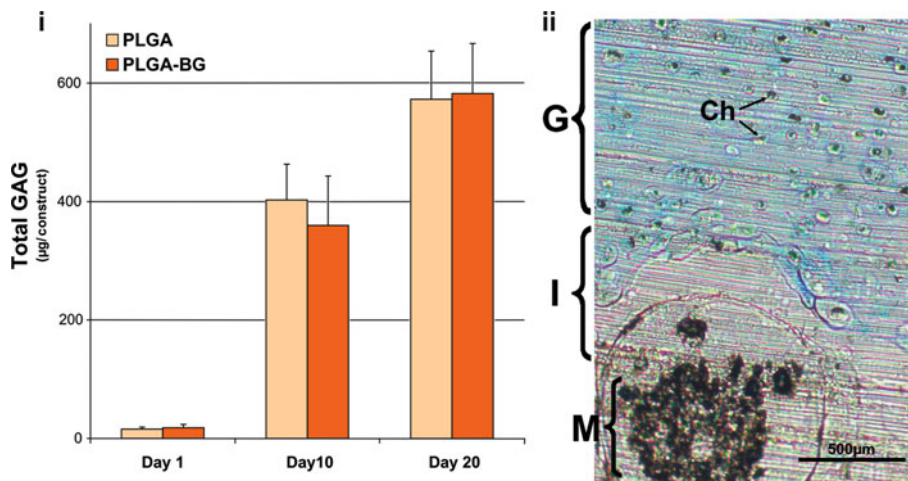

FIGURE 6. Proteoglycan deposition in stratified osteochondral scaffold. (i) Total GAG deposition increased over time with no significant difference observed between PLGA and PLGA-BG groups. (ii) a GAG-rich matrix was evident in the gel-only region and the interface region with the hydrogel penetrating into the pores of the microsphere scaffold (Alcian Blue stain, Day 10; 20×).
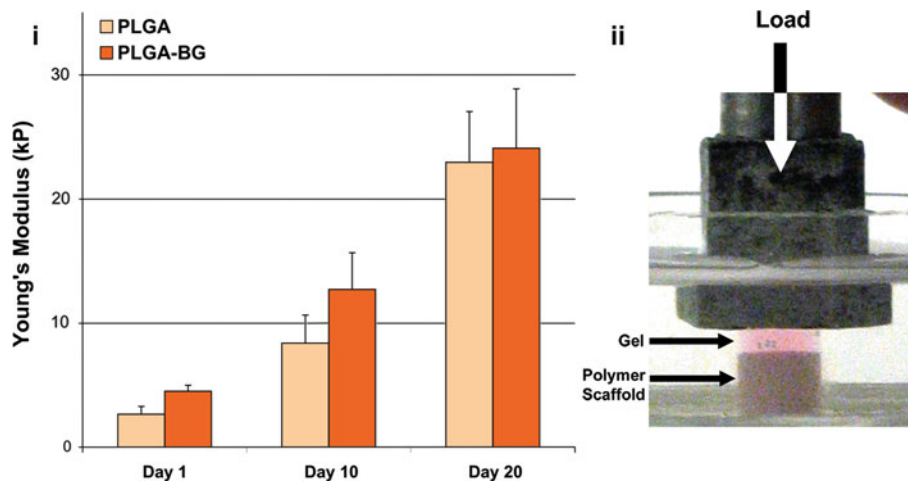

FIGURE 7. Mechanical property. (i) Equilibrium Young's modulus of the construct increased with time, doubling about every 10 days and reached up to ~25 kPa at day 20. No difference was found between the PLGA and PLGA-BG groups. (ii) Mechanical testing apparatus.
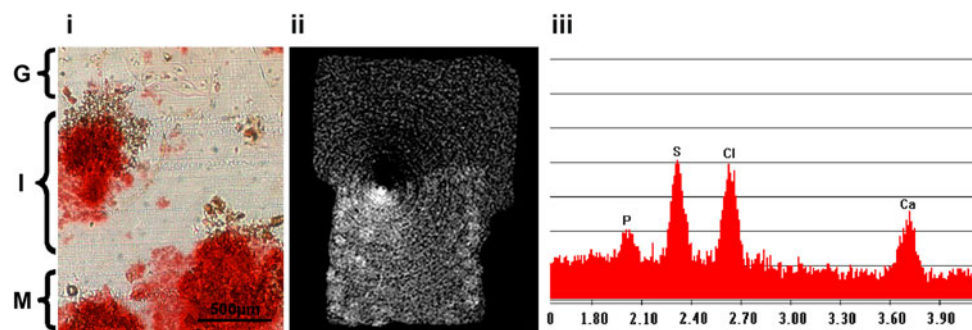
FIGURE 8. Mineral distribution in Stratified osteochondral scaffold. A mineralized matrix was only detected in the PLGA-BG group, localized at the interface and bone regions of the osteochondral graft: (i) Alizarin Red S (Day 10. 20×), (ii) micro-CT (bright white area positive for mineral) and (iii) energy dispersive X-ray analysis (EDAX), note the distinct Ca, P and S peaks.

Evaluation of mineral deposition revealed that calcification was not observed as no mineralization was seen in grafts fabricated with PLGA microspheres (data not shown). In contrast, both Alizarin Red staining (Fig. 8i) and micro-CT analysis (Fig. 8ii) revealed that a mineralized matrix was present in the osteochondral scaffolds with interface and bone regions consisting of PLGA-BG microspheres. As shown in Fig. 8i, a calcified matrix was evident within the microsphere (M) region as well as at the interface (I) in constructs formed with PLGA-BG. This observation was confirmed with EDAX analysis (Fig. 8iii) that revealed the presence of Ca, P peaks associated with mineral presence, as well as a strong sulfur peak that is commonly associated with protein deposition.

DISCUSSION

This study focuses on the design and optimization of a novel tissue engineered osteochondral graft for integrative cartilage repair. Specifically, a multi-phased scaffold with PLGA-BG composite microspheres and hydrogel was developed, and it supported the simultaneous co-culture of chondrocytes and osteoblasts that led to the formation of three distinct yet continuous regions of cartilage, calcified cartilage and bone-like matrices. It was found that higher chondrocyte density in the hydrogel region enhanced extracellular matrix deposition and mechanical properties of the graft over time, with 60 million cells/mL being the most optimal density tested in the hydrogel region. At the interface region, the hydrogel + PLGA-BG composite supported chondrocyte growth and phenotype, with the PLGA-BG phase enhancing both proteoglycans deposition and the mineralization potential of chondrocytes, as evident in the significant ALP activity measured when compared to PLGA alone. Consequently, the presence of BG in the graft promoted Ca-P deposition in the interface and bone regions of

the graft. It is important to note that the stability of the stratified scaffold was sustained *in vitro*, with no delamination observed between the scaffold regions, that continuity was maintained between scaffold phases and that spatial control over cell distribution was evident in the cell-tracking studies.

The stratified osteochondral graft based on PLGA-BG composite microspheres and hydrogel consisted of a gel-only region for chondrogenesis (G), a microsphere-only region for osteogenesis (M), and a combined region of gel and microspheres for the development of an osteochondral interface (I). It was observed that the chondrocyte-laden agarose hydrogel phase of the graft promoted the formation of the proteoglycan-rich matrix. It is well established that chondrocytes embedded in agarose maintain their phenotype and develop a functional cartilage-like extracellular matrix in free-swelling culture.[9,15,16,51,52] The chondrocyte-seeded interface region with hydrogel and PLGA-BG microspheres supported the formation of a mineralized matrix within the proteoglycans- and collagen-rich matrix. The microsphere-only phase of the graft intended for bone regeneration supported the growth and collagen deposition by osteoblasts.

It is observed here that the incorporation of BG in the PLGA microspheres facilitated mineral formation at both the interface and bone regions compared to PLGA alone. Moreover, the PLGA-BG composite microsphere induced an increase in ALP activity of chondrocytes which suggests that it could facilitate cell-mediated production of a mineralized cartilage matrix at the interface region. Previous studies have also found the PLGA-BG composite to be biocompatible, osteoconductive, and osteointegrative.[46] This is not surprising as BG is considered to be the most bone-bioactive or osteointegrative material known to date.[31] Published studies evaluating BG as a bone graft showed improved implant to host integration compare to calcium phosphate-based ceramic materials such as hydroxyapatite or tri-calcium phosphate.[31,32] The

findings of this study demonstrate that the stratified scaffold design coupled with spatial control of osteoblast-chondrocyte interactions promoted the development of controlled biomimetic heterogeneity on the graft.

In this study, the calcified interface region was pre-incorporated into graft design by the inclusion of a mineralized scaffold phase (PLGA-BG) infused with chondrocyte-laden agarose hydrogel. Although a calcified matrix was observed at the interface region of our graft, at this time it is not possible to distinguish cell-mediated mineralization from that of the inherent transformation of the BG surface into calcium phosphate. It is however encouraging that chondrocytes seeded directly on PLGA-BG microsphere exhibited significantly higher ALP activity. In addition, while this study did not determine the expression of hypertrophic markers, Khanarian et al. reported the upregulation of type X collagen by chondrocytes when cultured in agarose hydrogel with BG particles.[40] Future studies will investigate the development of chondrocyte hypertrophy at the interface region of the stratified scaffold.

The formation of a calcified cartilage-like zone has also been investigated by other groups, where deep zone chondrocytes were directly seeded on a calcium polyphosphate scaffold.[5] As the cartilaginous tissue forms, the chondrocytes infiltrated into the superficial region of the calcium polyphosphate scaffold, resulting in three distinct regions—cartilage, mineralized cartilage, and a GAG-rich layer directly above the bone scaffold. The presence of this cell-mediated mineralized cartilage layer has been shown to increase both the compressive mechanical properties of the tissue engineered cartilage, as well as the interfacial shear strength of the graft.[6] More recently, using both collagen-glycosaminoglycan-based scaffolds, Harley et al. reported on the design of an osteochondral scaffold with cartilage and bone regions as well as a continuous osteochondral interface-like region in between these two phases.[27] While the potential of this collagen-GAG scaffold system for simultaneous cartilage, interface or bone tissue formation remains to be tested in vitro and in vivo, it is apparent that stratified design with pre-integrated cartilage-interface-bone regions is a promising approach to functional and integrative cartilage repair.

It was observed here that the osteochondral graft supported the simultaneous growth of chondrocytes and osteoblasts, while maintaining an integrated and continuous structure throughout the study. In addition, chondrocytes in the cartilage region produced a proteoglycan-rich matrix while osteoblasts in the bone region produced a mineralized collagen-rich matrix. These findings are consistent with our published study

where osteoblasts and chondrocytes were co-cultured in a monolayer-over-micromass model.[38] During co-culture, both chondrocytes and osteoblasts maintained their respective phenotype, where chondrocytes continued to produce proteoglycans and type II collagen while osteoblasts produced type I collagen and maintained ALP activity.

To optimize our design, this study also examined the effects of chondrocyte density on matrix deposition and mechanical properties. As expected, an increase in chondrocyte density corresponded to elevated extracellular matrix deposition and increased mechanical properties of the graft under free-swelling conditions. These findings are consistent with previously published reports evaluating the response of chondrocytes embedded in hydrogel. We observed a decrease in cell number in all of our constructs with the highest decrease seen in 60 million chondrocyte/mL group. This is also consistent with other published results[51] where chondrocytes embedded in agarose usually do not proliferate due to spatial constraint and usually exhibit some cell death due to altered nutrient transport to the center of the construct. Constructs seeded with 60 million/mL measured significantly higher young's modulus, proteoglycan and collagen deposition after four weeks of culture.[52] Therefore, the osteochondral grafts tested in this study were seeded with 60 million/mL, and both collagen and GAG content within the graft as well as the mechanical properties of the cartilage phase increased with culturing time. To further optimize our graft system, future studies will evaluate the effect of osteoblast seeding density on matrix deposition during co-culture.

The primary rationale for encapsulating chondrocytes in agarose for the cartilage region over other methods such as seeding chondrocytes directly onto a bone graft[5,83] is due to the improved mechanical strength that can be achieved. Nonetheless, the highest modulus achieved in this study was about 20 kPa, which is still considerably lower compared to native cartilage.[7,53,54] It has been reported that combination of dynamic loading and growth factor stimulation can produce agarose-based tissue engineered cartilage graft with comparable mechanical properties as those of native cartilage.[45] Therefore, future studies will focus on utilizing biochemical factors and mechanical stimuli to improve graft mechanical properties. Additional planned studies include optimizing the multi-phased scaffold to develop osteochondral grafts with a physiologically relevant interface, by investigating in detail the effect of BG on chondrocyte-mediated mineralization and hypertrophy. In addition, while higher GAG deposition was observed when chondrocytes were seeded directly on PLGA-BG microspheres, no apparent difference in GAG was evident histologically

between the interface and gel-only regions of the scaffold, likely due to the fact that at the interface region, the chondrocytes were encapsulated in the hydrogel instead of being directly exposed to PLGA-BG. Therefore, to improve chondrocyte interaction with PLGA-BG, agarose may be added to the hydrogel to promote degradation of agarose matrix[55] in conjunction with increasing hydrogel porosity. Moreover, although the strength of the interface region was not in this current study, we plan to perform shear tests to better define integration and characterize the mechanical properties of the interface in future studies.[5]

CONCLUSIONS

This study demonstrated the successful development of an osteochondral graft *in vitro* with biomimetic multi-tissue regions, including a pre-designed and pre-integrated interface region. The scaffold was optimized for both cell density and microsphere composition. Controlled chondrocyte and osteoblast culture on each scaffold region resulted in the formation of three distinct yet continuous regions of cartilage, calcified cartilage and bone-like matrices. Future studies will focus on further optimization of the functional properties of the stratified osteochondral scaffold and *in vivo* evaluations. It is emphasized that the interface tissue engineering strategies delineated here are applicable to the regeneration of other soft tissue-to-bone interfaces, and are anticipated to have a significant impact on integrative soft tissue repair.

ACKNOWLEDGMENT

REFERENCES

[1]Ahsan, T., L. M. Lottman, F. Harwood, D. Amiel, and R. L. Sah. Integrative cartilage repair: inhibition by beta-aminopropionitrile. *J. Orthop. Res.* 17:850–857, 1999.

[2]Akizuki, S., Y. Yasukawa, and T. Takizawa. A new method of hemostasis for cementless total knee arthroplasty. *Bull. Hosp. Jt. Dis.* 56:222–224, 1997.

[3]Alhadlaq, A., and J. J. Mao. Tissue-engineered neogenesis of human-shaped mandibular condyle from rat mesenchymal stem cells. *J. Dent. Res.* 82:951–956, 2003.

[4]Alhadlaq, A., and J. J. Mao. Tissue-engineered osteochondral constructs in the shape of an articular condyle. *J. Bone Joint Surg. Am.* 87:936–944, 2005.

[5]Allan, K. S., R. M. Pilliar, J. Wang, M. D. Grynpas, and R. A. Kandel. Formation of biphasic constructs containing cartilage with a calcified zone interface. *Tissue Eng.* 13:167–177, 2007.

[6]Angele, P., R. Kujat, M. Nerlich, J. Yoo, V. Goldberg, and B. Johnstone. Engineering of osteochondral tissue with bone marrow mesenchymal progenitor cells in a derivatized hyaluronan-gelatin composite sponge. *Tissue Eng.* 5:545–554, 1999.

[7]Athanasiou, K. A., M. P. Rosenwasser, J. A. Buckwalter, T. I. Malinin, and V. C. Mow. Interspecies comparisons of in situ intrinsic mechanical properties of distal femoral cartilage. *J. Orthop. Res.* 9:330–340, 1991.

[8]Beiser, I. H., and I. O. Kanat. Subchondral bone drilling: a treatment for cartilage defects. *J. Foot Surg.* 29:595–601, 1990.

[9]Benya, P. D., and J. D. Shaffer. Dedifferentiated chondrocytes reexpress the differentiated collagen phenotype when cultured in agarose gels. *Cell* 30:215–224, 1982.

[10]Boccaccini, A. R., and J. J. Blaker. Bioactive composite materials for tissue engineering scaffolds. *Expert Rev. Med. Devices* 2:303–317, 2005.

[11]Bullough, P. G. The geometry of diarthrodial joints, its physiologic maintenance, and the possible significance of age-related changes in geometry-to-load distribution and the development of osteoarthritis. *Clin. Orthop. Relat Res.* 61–66, 1981.

[12]Bullough, P. G. The role of joint architecture in the etiology of arthritis. *Osteoarthr. Cartil.* 12(Suppl A):S2–S9, 2004.

[13]Bullough, P. G., and A. Jagannath. The morphology of the calcification front in articular cartilage. Its significance in joint function. *J. Bone Joint Surg. Br.* 65:72–78, 1983.

[14]Burr, D. B. Anatomy and physiology of the mineralized tissues: Role in the pathogenesis of osteoarthrosis. *Osteoarthr. Cartil.* 12(Suppl A):S20–S30, 2004.

[15]Buschmann, M. D., Y. A. Gluzband, A. J. Grodzinsky, and E. B. Hunziker. Mechanical compression modulates matrix biosynthesis in chondrocyte/agarose culture. *J. Cell Sci.* 108(Pt 4):1497–1508, 1995.

[16]Buschmann, M. D., Y. A. Gluzband, A. J. Grodzinsky, J. H. Kimura, and E. B. Hunziker. Chondrocytes in agarose culture synthesize a mechanically functional extracellular matrix. *J. Orthop. Res.* 10:745–758, 1992.

[17]Cao, T., K. H. Ho, and S. H. Teoh. Scaffold design and in vitro study of osteochondral coculture in a three-dimensional porous polycaprolactone scaffold fabricated by fused deposition modeling. *Tissue Eng.* 9(Suppl 1):S103–S112, 2003.

[18]Chowdhury, T. T., D. L. Bader, and D. A. Lee. Dynamic compression counteracts il-1 beta-induced release of nitric oxide and pge2 by superficial zone chondrocytes cultured in agarose constructs. *Osteoarthr. Cartil.* 11:688–696, 2003.

[19]Collins, D. H. The Pathology of Articular and Spinal Diseases. Baltimore, MD: William & Wilkins, 1950.

[20]D'Lima, D. D., S. Hashimoto, P. C. Chen, C. W. Colwell, Jr., and M. K. Lotz. Impact of mechanical trauma on matrix and cells. *Clin. Orthop. Relat Res.* S90–S99, 2001.

[21]Elisseeff, J., C. Puleo, F. Yang, and B. Sharma. Advances in skeletal tissue engineering with hydrogels. *Orthod. Craniofac. Res.* 8:150–161, 2005.

[22]Fawns, H. T., and J. W. Landells. Histochemical studies of rheumatic conditions. I. Observations on the fine structures of the matrix of normal bone and cartilage. *Ann. Rheum. Dis.* 12:105–113, 1953.

[23]Frenkel, S. R., G. Bradica, J. H. Brekke, S. M. Goldman, K. Ieska, P. Issack, M. R. Bong, H. Tian, J. Gokhale, R. D. Coutts, and R. T. Kronengold. Regeneration of articular cartilage-evaluation of osteochondral defect repair in the rabbit using multiphasic implants. *Osteoarthr. Cartil.* 13:798–807, 2005.

[24]Gao, J., J. E. Dennis, L. A. Solchaga, A. S. Awadallah, V. M. Goldberg, and A. I. Caplan. Tissue-engineered fabrication of an osteochondral composite graft using rat bone marrow-derived mesenchymal stem cells. *Tissue Eng.* 7:363–371, 2001.

[25]Gao, J., J. E. Dennis, L. A. Solchaga, V. M. Goldberg, and A. I. Caplan. Repair of osteochondral defect with tissue-engineered two-phase composite material of injectable calcium phosphate and hyaluronan sponge. *Tissue Eng.* 8:827–837, 2002.

[26]Hangody, L., G. Kish, Z. Karpati, I. Szerb, and I. Udvarhelyi. Arthroscopic autogenous osteochondral mosaicplasty for the treatment of femoral condylar articular defects. A preliminary report. *Knee Surg. Sports Traumatol. Arthrosc.* 5:262–267, 1997.

[27]Harley, B. A., A. K. Lynn, Z. Wissner-Gross, W. Bonfield, I. V. Yannas, and L. J. Gibson. Design of a multiphase osteochondral scaffold iii: fabrication of layered scaffolds with continuous interfaces. *J. Biomed. Mater. Res. A* 92:1078–1093.

[28]Harper, M. C. Viscous isoamyl 2-cyanoacrylate as an osseous adhesive in the repair of osteochondral osteotomies in rabbits. *J. Orthop. Res.* 6:287–292, 1988.

[29]Havelka, S., V. Horn, D. Spohrova, and P. Valouch. The calcified-noncalcified cartilage interface: the tidemark. *Acta Biol. Hung.* 35:271–279, 1984.

[30]Haynes, D. W. The mineralization front of articular cartilage. *Metab. Bone Dis. Rel. Res.* 2(suppl):55–59, 1980.

[31]Hench, L. L. Bioceramics: from concept to clinic. *J. Am. Ceram. Soc.* 74(7):1487–1510, 1991.

[32]Hench, L. L., and J. M. Polak. Third-generation biomedical materials. *Science* 295:1014–1017, 2002.

[33]Holland, T. A., E. W. Bodde, L. S. Baggett, Y. Tabata, A. G. Mikos, and J. A. Jansen. Osteochondral repair in the rabbit model utilizing bilayered, degradable oligo(poly (ethylene glycol) fumarate) hydrogel scaffolds. *J. Biomed. Mater. Res. A* 75:156–167, 2005.

[34]Hung, C. T., E. G. Lima, R. L. Mauck, E. Taki, M. A. LeRoux, H. H. Lu, R. G. Stark, X. E. Guo, and G. A. Ateshian. Anatomically shaped osteochondral constructs for articular cartilage repair. *J. Biomech.* 36:1853–1864, 2003.

[35]Hunziker, E. B., and I. M. Driesang. Functional barrier principle for growth-factor-based articular cartilage repair. *Osteoarthr. Cartil.* 11:320–327, 2003.

[36]Hunziker, E. B., I. M. Driesang, and C. Saager. Structural barrier principle for growth factor-based articular cartilage repair. *Clin. Orthop. Relat. Res.* S182–S189, 2001.

[37]Jackson, D. W., M. J. Scheer, and T. M. Simon. Cartilage substitutes: overview of basic science and treatment options. *J. Am. Acad. Orthop. Surg.* 9:37–52, 2001.

[38]Jiang, J., S. B. Nicoll, and H. H. Lu. Co-culture of osteoblasts and chondrocytes modulates cellular differentiation in vitro. *Biochem. Biophys. Res. Commun.* 338:762–770, 2005.

[39]Kandel, R. A., M. Grynpas, R. Pilliar, J. Lee, J. Wang, S. Waldman, P. Zalzal, and M. Hurtig. Repair of osteochondral defects with biphasic cartilage-calcium polyphosphate constructs in a sheep model. *Biomaterials* 27:4120–4131, 2006.

[40]Khanarian, N. T., S. A. McArdle, and H. H. Lu. Effects of 45s5 bioactive glass particles on chondrocyte biosynthesis and mineralization. *Society for Biomaterials Proceedings*, 2009.

[41]Kim, Y. J., R. L. Sah, J. Y. Doong, and A. J. Grodzinsky. Fluorometric assay of DNA in cartilage explants using hoechst 33258. *Anal. Biochem.* 174:168–176, 1988.

[42]Lane, L. B., and P. G. Bullough. Age-related changes in the thickness of the calcified zone and the number of tidemarks in adult human articular cartilage. *J. Bone Jt. Surg. Br.* 62:372–375, 1980.

[43]Lemperg, R. The subchondral bone plate of the femoral head in adult rabbits. I. Spontaneus remodelling studied by microradiography and tetracycline labelling. *Virchows Arch. A Pathol. Pathol. Anat.* 352:1–13, 1971.

[44]Lethbridge-Cejku, M., J. S. Schiller, and L. Bernadel. Summary health statistics for U.S. adults: National Health Interview Survey, 2002. *Vital Health Stat.* 10.222:1–151, 2004.

[45]Lima, E. G., L. Bian, K. W. Ng, R. L. Mauck, B. A. Byers, R. S. Tuan, G. A. Ateshian, and C. T. Hung. The beneficial effect of delayed compressive loading on tissue-engineered cartilage constructs cultured with tgf-beta3. *Osteoarthr. Cartil.* 15:1025–1033, 2007.

[46]Lu, H. H., S. F. El Amin, K. D. Scott, and C. T. Laurencin. Three-dimensional, bioactive, biodegradable, polymer-bioactive glass composite scaffolds with improved mechanical properties support collagen synthesis and mineralization of human osteoblast-like cells in vitro. *J. Biomed. Mater. Res.* 64A:465–474, 2003.

[47]Lu, H. H., J. M. Vo, J. Lin, S. Shin, R. Cozin, R. Tsay, and R. Landesberg. Controlled delivery of growth factors derived from platelet-rich plasma for bone formation. *J. Biomed. Mater. Res. A* 86A(4):1128–1136, 2008.

[48]Lu, H. H., A. Tang, S. C. Oh, J. P. Spalazzi, and K. Dionisio. Compositional effects on the formation of a calcium phosphate layer and the response of osteoblast-like cells on polymer-bioactive glass composites. *Biomaterials* 26:6323–6334, 2005.

[49]Lyons, T. J., R. W. Stoddart, S. F. McClure, and J. McClure. The tidemark of the chondro-osseous junction of the normal human knee joint. *J. Mol. Histol.* 36:207–215, 2005.

[50]Matava, M. J., and P. A. Hughes. Removal of a retained herbert-whipple screw with use of the osteochondral autograft transfer system (oats) core harvester: a case report. *Am. J. Orthop.* 33:598–601, 2004.

[51]Mauck, R. L., S. L. Seyhan, G. A. Ateshian, and C. T. Hung. Influence of seeding density and dynamic deformational loading on the developing structure/function relationships of chondrocyte-seeded agarose hydrogels. *Ann. Biomed. Eng.* 30:1046–1056, 2002.

[52]Mauck, R. L., C. C. Wang, E. S. Oswald, G. A. Ateshian, and C. T. Hung. The role of cell seeding density and nutrient supply for articular cartilage tissue engineering with deformational loading. *Osteoarthr. Cartil.* 11:879–890, 2003.

[53]Mow, V. C., W. Y. Gu, F. H. Chen, and R. Huiskes. Structure and function of articular cartilage and meniscus. In: Basic Orthopaedic Biomechanics and Mechano-biology. Philadelphia: Lippincott Williams and Wilkins, 2007, pp. 181–258.

[54]Mow, V. C., C. S. Proctor, M. A. Kelly, M. Nordin, H. F. Victor, and K. Forssen. Biomechanics of articular cartilage. In: Basic Biomechanics of the Musculoskeletal System. Philadelphia, PA: Lea and Febiger, 1989, pp. 31–58.

[55]Ng, K. W., L. E. Kugler, S. B. Doty, G. A. Ateshian, and C. T. Hung. Scaffold degradation elevates the collagen content and dynamic compressive modulus in engineered articular cartilage. *Osteoarthr. Cartil.* 17:220–227, 2009.

[56]Ng, K. W., E. G. Lima, L. Bian, C. J. O'Conor, P. S. Jayabalan, A. M. Stoker, K. Kuroki, C. R. Cook, G. A. Ateshian, J. L. Cook, and C. T. Hung. Passaged adult chondrocytes can form engineered cartilage with functional mechanical properties: a canine model. *Tissue Eng. A* 16:1041–1051, 2009.

[57]Niederauer, G. G., M. A. Slivka, N. C. Leatherbury, D. L. Korvick, H. H. Harroff, W. C. Ehler, C. J. Dunn, and K. Kieswetter. Evaluation of multiphase implants for repair of focal osteochondral defects in goats. *Biomaterials* 21:2561–2574, 2000.

[58]O'Driscoll, S. W., F. W. Keeley, and R. B. Salter. The chondrogenic potential of free autogenous periosteal grafts for biological resurfacing of major full-thickness defects in joint surfaces under the influence of continuous passive motion. An experimental investigation in the rabbit. *J. Bone Jt. Surg. Am.* 68:1017–1035, 1986.

[59]Ochi, M., Y. Uchio, M. Tobita, and M. Kuriwaka. Current concepts in tissue engineering technique for repair of cartilage defect. *Artif. Organs* 25:172–179, 2001.

[60]Oegema, Jr., T. R., R. J. Carpenter, F. Hofmeister, and R. C. Thompson, Jr. The interaction of the zone of calcified cartilage and subchondral bone in osteoarthritis. *Microsc. Res. Tech.* 37:324–332, 1997.

[61]Oegema, Jr., T. R., S. L. Johnson, T. Meglitsch, and R. J. Carpenter. Prostaglandins and the zone of calcified cartilage in osteoarthritis. *Am. J. Ther.* 3:139–149, 1996.

[62]Oegema, T. R., Jr., R. C. Thompson, Jr., and C.-G. K. Brandt. Cartilage-bone interface (tidemark). In: Cartilage Changes in Osteoarthritis. Indianapolis, IN: Indiana School of Medicine Publ., 1990, pp. 43–52.

[63]Oegema, T. R., Jr., R. C. Thompson, Jr., K. E. Kuettner, R. Schleyerbach, J. G. Peyron, and V. C. Hascall. The zone of calcified cartilage. Its role in osteoarthritis. In: Articular Cartilage and Osteoarthritis. New York, NY: Raven Press, 1992, pp. 319–331.

[64]Oettmeier, R., K. Abendroth, and S. Oettmeier. Analyses of the tidemark on human femoral heads. I. Histochemical, ultrastructural and microanalytic characterization of the normal structure of the intercartilaginous junction. *Acta Morphol. Hung.* 37:155–168, 1989.

[65]Radin, E. L., D. B. Burr, B. Caterson, D. Fyhrie, T. D. Brown, and R. D. Boyd. Mechanical determinants of osteoarthrosis. *Semin. Arthr. Rheum.* 21:12–21, 1991.

[66]Reddy, G. K., and C. S. Enwemeka. A simplified method for the analysis of hydroxyproline in biological tissues. *Clin. Biochem.* 29:225–229, 1996.

[67]Redler, I., V. C. Mow, M. L. Zimny, and J. Mansell. The ultrastructure and biomechanical significance of the tidemark of articular cartilage. *Clin. Orthop. Relat Res.* 112:357–362, 1975.

[68]Redman, S. N., S. F. Oldfield, and C. W. Archer. Current strategies for articular cartilage repair. *Eur. Cell Mater.* 9:23–32, 2005.

[69]Roberts, S. R., M. M. Knight, D. A. Lee, and D. L. Bader. Mechanical compression influences intracellular ca2+

[70]Schaefer, D., I. Martin, G. Jundt, J. Seidel, M. Heberer, A. Grodzinsky, I. Bergin, G. Vunjak-Novakovic, and L. E. Freed. Tissue-engineered composites for the repair of large osteochondral defects. *Arthr. Rheum.* 46:2524–2534, 2002.

[71]Schaefer, D., I. Martin, P. Shastri, R. F. Padera, R. Langer, L. E. Freed, and G. Vunjak-Novakovic. In vitro generation of osteochondral composites. *Biomaterials* 21:2599–2606, 2000.

[72]Schek, R. M., J. M. Taboas, S. J. Hollister, and P. H. Krebsbach. Tissue engineering osteochondral implants for temporomandibular joint repair. *Orthod. Craniofac. Res.* 8:313–319, 2005.

[73]Schek, R. M., J. M. Taboas, S. J. Segvich, S. J. Hollister, and P. H. Krebsbach. Engineered osteochondral grafts using biphasic composite solid free-form fabricated scaffolds. *Tissue Eng.* 10:1376–1385, 2004.

[74]Shao, X., J. C. Goh, D. W. Hutmacher, E. H. Lee, and G. Zigang. Repair of large articular osteochondral defects using hybrid scaffolds and bone marrow-derived mesenchymal stem cells in a rabbit model. *Tissue Eng.* 12:1539–1551, 2006.

[75]Sherwood, J. K., S. L. Riley, R. Palazzolo, S. C. Brown, D. C. Monkhouse, M. Coates, L. G. Griffith, L. K. Landeen, and A. Ratcliffe. A three-dimensional osteochondral composite scaffold for articular cartilage repair. *Biomaterials* 23:4739–4751, 2002.

[76]Singh, S., C. C. Lee, and B. K. Tay. Results of arthroscopic abrasion arthroplasty in osteoarthritis of the knee joint. *Singapore Med. J.* 32:34–37, 1991.

[77]Sledge, S. L. Microfracture techniques in the treatment of osteochondral injuries. *Clin. Sports Med.* 20:365–377, 2001.

[78]Solchaga, L. A., J. Gao, J. E. Dennis, A. Awadallah, M. Lundberg, A. I. Caplan, and V. M. Goldberg. Treatment of osteochondral defects with autologous bone marrow in a hyaluronan-based delivery vehicle. *Tissue Eng.* 8:333–347, 2002.

[79]Solchaga, L. A., J. S. Temenoff, J. Gao, A. G. Mikos, A. I. Caplan, and V. M. Goldberg. Repair of osteochondral defects with hyaluronan- and polyester-based scaffolds. *Osteoarthr. Cartil.* 13:297–309, 2005.

[80]Spalazzi, J. P., K. L. Dionisio, J. Jiang, and H. H. Lu. Osteoblast and chondrocyte interactions during coculture on scaffolds. *IEEE Eng. Med. Biol. Mag.* 22:27–34, 2003.

[81]Teixeira, C. C., M. Hatori, P. S. Leboy, M. Pacifici, and I. M. Shapiro. A rapid and ultrasensitive method for measurement of DNA, calcium and protein content, and alkaline phosphatase activity of chondrocyte cultures. *Calcif. Tissue Int.* 56:252–256, 1995.

[82]Thambyah, A. A hypothesis matrix for studying biomechanical factors associated with the initiation and progression of posttraumatic osteoarthritis. *Med. Hypotheses* 64:1157–1161, 2005.

[83]Tuli, R., S. Nandi, W. J. Li, S. Tuli, X. Huang, P. A. Manner, P. Laquerriere, U. Noth, D. J. Hall, and R. S. Tuan. Human mesenchymal progenitor cell-based tissue engineering of a single-unit osteochondral construct. *Tissue Eng.* 10:1169–1179, 2004.